Teleoperation of an ankle-foot prosthesis with a wrist exoskeleton

Cara G. Welker[1,2], Vincent L. Chiu[2], Alexandra S. Voloshina[2], Steven H. Collins[2], and Allison M. Okamura[2]

***Abstract*—Objective: We aimed to develop a system for people with amputation that non-invasively restores missing control and sensory information for an ankle-foot prosthesis. Methods: In our approach, a wrist exoskeleton allows people with amputation to control and receive feedback from their prosthetic ankle via teleoperation. We implemented a position control scheme and torque control scheme, both of which provide haptic feedback at the wrist. We also investigated two low-level position controllers, and measured tracking error and frequency response for each system component. To demonstrate feasibility and evaluate system performance, we conducted an experiment in which one participant with a transtibial amputation tracked desired wrist trajectories during walking, while we measured wrist and ankle response. Results: Benchtop testing demonstrated that for relevant walking frequencies, system error was below human perception error. During the walking experiment, the participant was able to voluntarily follow different wrist trajectories with an average RMS error of 1.55° after training. A position control scheme using feedforward control with iterative learning and haptic feedback at the wrist resulted in the most accurate ankle tracking (RMS error = 0.8°). The torque control scheme achieved an ankle torque RMS error of 8.3 N·m. Conclusion: We present a system that allows a user with amputation to control an ankle-foot prosthesis and receive feedback about its state using a wrist exoskeleton with accuracy comparable to biological neuromotor control. Significance: This bilateral teleoperation system enables novel prosthesis control and feedback strategies that could result in improved prosthesis control and aid motor learning.**

***Index Terms*—Amputation, Exoskeleton, Teleoperation**

I. Introduction

MORE than 600,000 people live with major lower-limb amputation in the United States, a number that is expected to double by 2050 given the rising rates of vascular disease that lead to amputation [1]. As the primary cause of amputation in the US, vascular disease leads to reduced aerobic capacity and makes even slow walking a demanding task [2]. Those walking with conventional passive prosthetic limbs expend 20-47% more energy and have slower self-selected walking speeds compared to unimpaired individuals [3], [4]. Walking fatigue is second only to residual limb pain among concerns of those with lower limb amputation [5]. Limited mobility results in numerous secondary health problems and loss of independence, increasing medical costs and reliance on caregivers [6]. Additionally, although the average age of people with amputation is only 50 years old [7], 50% experience at least one fall annually [8], compared to the less than 30% of the elderly population above 65 years old with intact limbs who fall once a year [9]. Finally, individuals with lower limb amputation also have an increased risk of osteoarthritis in their sound knee and hip due to increased reliance on the intact joints [10], [11].

As evidenced by the number of issues faced by people with amputation, lower limb loss disrupts not only normal motor function, but also many sensory pathways. The human ankle, for example, is a complex joint comprised of rigid bones, passive tendons, muscle actuators, and sensory components, including muscle spindles and Golgi Tendon organs that relay information about the orientation and force production at the joint. Inputs to and from the central nervous system are also important, as the brain receives a copy of motor commands sent to the muscles to more accurately predict where the joint is in space [12]. An internal model then maps motor commands to expected sensory consequences [13].

Despite the complex interplay between sensorimotor commands in the biological ankle, most commercial ankle-foot prostheses focus primarily on restoring motor function to the user and lack sensory feedback from the joint. Recently, it has been shown that sensory feedback from a prosthestic limb can allow the user to experience more ownership of their limb [14], as well as reduce task times, metabolic cost, and phantom limb pain [15], [16]. The sensory feedback provided in these studies is typically either in the form of simplistic binary cues, such as vibrotactile [14] or electrocutaneous stimulation [15], or invasive surgical procedures [16], [17]. Because there is evidence that continuous feedback can result in reduced task times compared to binary feedback [18], and surgical options are expensive and can result in complications, there is room for continued development of nonsurgical, continuous feedback methods for these devices. This type of feedback has been investigated for prosthetic hands by transmitting torque to a user's elbow [19] or force to a user's toes [20]. Providing continuous feedback from a lower-extremity prosthesis to an upper extremity during gait might provide the benefits of continuous feedback without an invasive surgery.

In addition to the lack of sensory feedback provided by the majority of lower limb prostheses, most commercial devices are passive and therefore lack the ability to provide the net work or power that the biological ankle does during walking. Several powered ankle-foot prostheses exist, and one has been shown to reduce the metabolic cost of walking under some circumstances [21], [22], but how best to control them remains an open question. Usually these devices attempt to mimic typical behavior of an intact ankle during walking. There is reason to believe that customization could improve on this control, because studies using human-in-the-loop optimization in healthy individuals have shown that small individualized changes in kinematics or kinetics of an exoskeleton can result in large changes in metabolic cost [23]. However, our unpublished

Departments of [1]Bioengineering and [2]Mechanical Engineering, Stanford University, Stanford, CA, 94305 USA. e-mail:cgwelker@stanford.edu

pilot studies using a similar approach to optimize prosthesis parameters have resulted in negligible changes in metabolic cost, perhaps because of the lack of sensory feedback. In addition, few studies have examined the benefits of providing the user with direct control over the movement of their lower limb prosthesis. Several surgical procedures, including targeted muscle reinnervation [24] and agonist-antagonist myoneural interfaces [25], show promise to improve control of prostheses in pilot studies, but these are invasive and expensive. The use of electromyography (EMG) from residual limb muscles as a command signal for the prosthesis has also been tested [26]–[28], but EMG sensors are inconsistent in day-to-day measurements and must be recalibrated frequently.

Teleoperation has been demonstrated as a highly effective way for people to directly control robotic devices when autonomy is not sufficient for the application [29]. Teleoperation allows for various combinations of force and position control pathways and feedback, and requirements for system stability are now well known [30], [31]. Studies have shown that teleoperation is effective in applications for upper-limb prostheses [32], in robot-assisted surgical systems [33], [34], and for rehabilitation, with information crossing between limbs [35]. Teleoperation of lower-limb exoskeletons has been investigated, but only in a virtual environment [36]. We propose to use a wrist exoskeleton to both teleoperate and receive sensory feedback about the state of a prosthetic ankle while walking (Figure 1). The wrist was chosen as the location for the feedback and control because of the neural link between wrist flexion and ankle flexion [37]. Such a system has the potential to improve user performance in terms of walking speed, balance, energy expenditure, and phantom limb pain.

The contributions of this work are: (1) the mechanical design of a wearable exoskeleton that is able to sense wrist angle and accurately transmit wrist flexion and extension torque, (2) the development of novel control strategies that allow a user with amputation to control an ankle-foot prosthesis and receive feedback about its state using the wrist exoskeleton, (3) benchtop tests characterizing the behavior of the wrist exoskeleton and ankle prosthesis, and (4) a feasibility study with a participant with amputation, quantifying the behavior of the system and the ability of the participant to voluntarily modulate ankle movements using the wrist exoskeleton during gait. Each contribution is addressed in further detail in the following sections.

II. System Design

Our system consists of an ankle-foot prosthesis emulator powered by off-board motors, a wrist exoskeleton, and a computer to control both devices (Figure 2A). The ankle-foot prosthesis emulator, described in further detail in Section 2B, was previously designed and tested [38] (Figure 2B). In addition, we built a one-degree-of-freedom wrist exoskeleton capable of interfacing with the ankle-foot prosthesis emulator (Figure 2C-2D). Our design goals were as follows. First, the wrist exoskeleton should be comfortable, lightweight, and backdrivable to allow for natural motion of the arm, as well as free motion of the wrist in flexion and extension. Second,

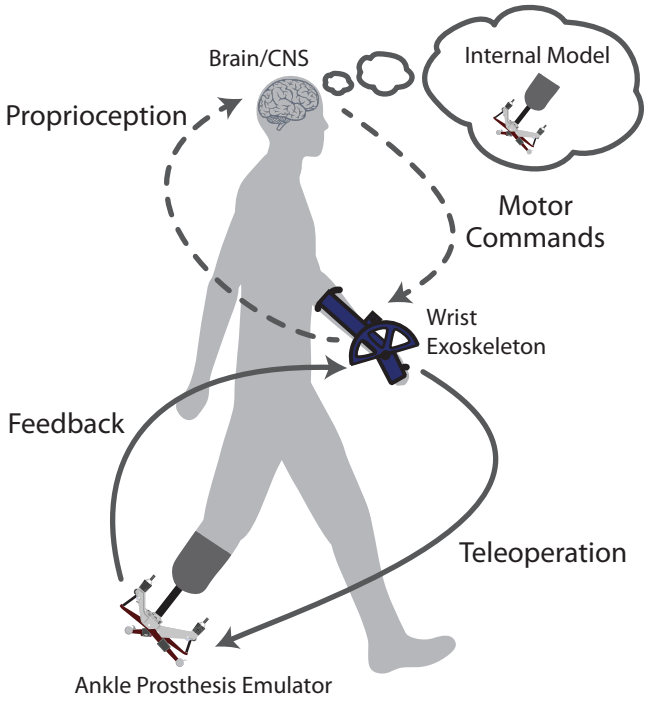

Fig. 1. The wrist exoskeleton allows the user to control the ankle prosthesis, as well as receive augmented sensory feedback about the ankle prosthesis' state, mimicking the control-feedback loop present in the unimpaired ankle. This augmented information being sent to the brain through the central nervous system (CNS) could allow the user to develop an internal model about the state of the ankle prosthesis and be able to better predict its motion.

it should be able to continuously transmit torques with an accuracy better than human wrist torque perception. Device torques should be noticeable to the user, but significantly lower than the user's maximum wrist flexion and extension torque, for both safety and to give the user the ability to easily overpower the transmitted torques to prevent fatigue. Third, it should accurately measure wrist angle within the resolution of human proprioception. Our system achieved all design goals.

A. Exoskeleton Design

The wrist exoskeleton is comprised of a forearm base and a hand base, with rigid links positioned on either side of the user's arm (Figure 2D). Both are attached to the arm with velcro straps, and the hand base is also grounded to the palm with a plate on the ventral side. To account for varying anthropometry of the forearm, spacers of different sizes can be attached to the inner portion of the wrist exoskeleton. All base components were 3D printed from polylactic acid (PLA).

The wrist exoskeleton uses a capstan drive transmission, which provides the required torque while maintaining backdrivability. The capstan drive transmits torque via a flexible, inextensible cable from a grooved capstan, which is attached to the motor shaft, to a sector pulley (Figure 2C). The torque is amplified by the ratio of the capstan to the sector pulley radius. We chose 1 N·m as our target maximum torque based on values of maximum isometric torque capabilities and human torque perception in wrist flexion and extension. Because

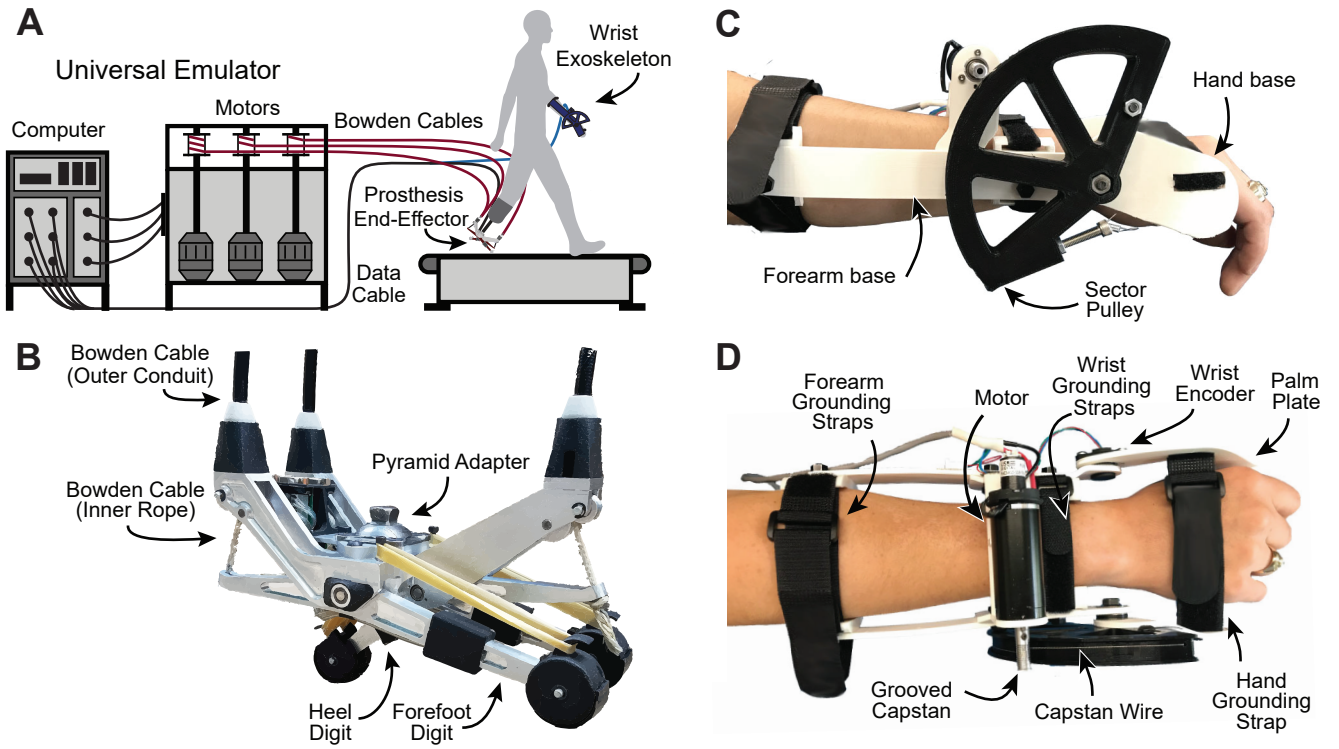

Fig. 2. A. Schematic of the system containing the ankle-prosthesis emulator with off-board motors, the wrist exoskeleton, the user, and the computer that runs the controller. B. Position of the three digits of the ankle-foot prosthesis emulator is dictated by the tension from Bowden cables. C. Side view of the wrist exoskeleton shows that it is comprised of three separate, 3D-printed parts. D. Top view of the wrist exoskeleton shows the capstan motor drive, encoder, and grounding to the user's arm.

the average human is capable of 4.6 N·m of isometric wrist extension torque and 6 N·m of isometric wrist flexion torque [39], our desired maximum torque is small enough that the user can easily overpower the exoskeleton. Perception of wrist flexion and extension torque has been characterized as a just noticeable difference that varies depending on the applied torque. With a maximum applied torque of 1 N·m, humans can detect a 20-30% change [40]. The exoskeleton is driven by an RE-25 motor (Maxon Motor, Switzerland) and a capstan ratio of 27 from the capstan pulley to the sector pulley diameter. We built a custom capstan pulley with grooved slots to minimize capstan wire slip.

The last two design requirements are related to wrist angle sensor resolution and wrist range of motion allowed by the device. The range of motion of the device is a function of the sector pulley arc length. We chose an arc length that allows the user to achieve 75° of wrist flexion and extension, similar to a typical range of motion [41]. An RM08 encoder (RLS, Slovenia) measures wrist angle with a resolution of 0.18° over 180° of motion. Studies of human wrist proprioceptive resolution have reported values between 1.33° and 4.64° for flexion and extension [42]–[44], so the exoskeleton has significantly greater angle resolution sensing than humans.

The exoskeleton weighs 363 grams. To reduce interference with arm swing, we placed the capstan drive on the dorsal and lateral sides of the arm, which are furthest from the torso during natural arm swing. With this design, users are able to swing their arms naturally while wearing the wrist exoskeleton.

B. Ankle Prosthesis Emulator

This wrist exoskeleton interfaces with an ankle-foot prosthesis emulator previously described in [38] (Figure 2A-2B). The prosthesis emulator is a 3-DOF device with one heel and two forefoot digits, with a maximum plantarflexion and dorsiflexion angle of 19°. The device weighs 1.2 kg, and is capable of supplying 140 N·m of torque at the toes and 100 N·m of torque at the heel, using off-board motors (Kollmorgen Corp, Maryland, USA) that power the device via Bowden cables. This device is equipped with both an encoder and a strain gauge at each digit to measure angle and torque.

III. System Control

We developed and tested two different control schemes: (1) position control with torque feedback and (2) torque control with a virtual spring. We also tested two low-level controllers within the position control scheme. Figure 3 provides an overview of all controllers tested, and Table 1 provides a description for the symbols used in the following section. All control was done with a real-time target machine (Speedgoat, Switzerland) sampling at 1000 Hz.

A. Position Control with Torque Feedback

In this control scheme, the user controls the position of the ankle using the wrist to provide the reference input, while

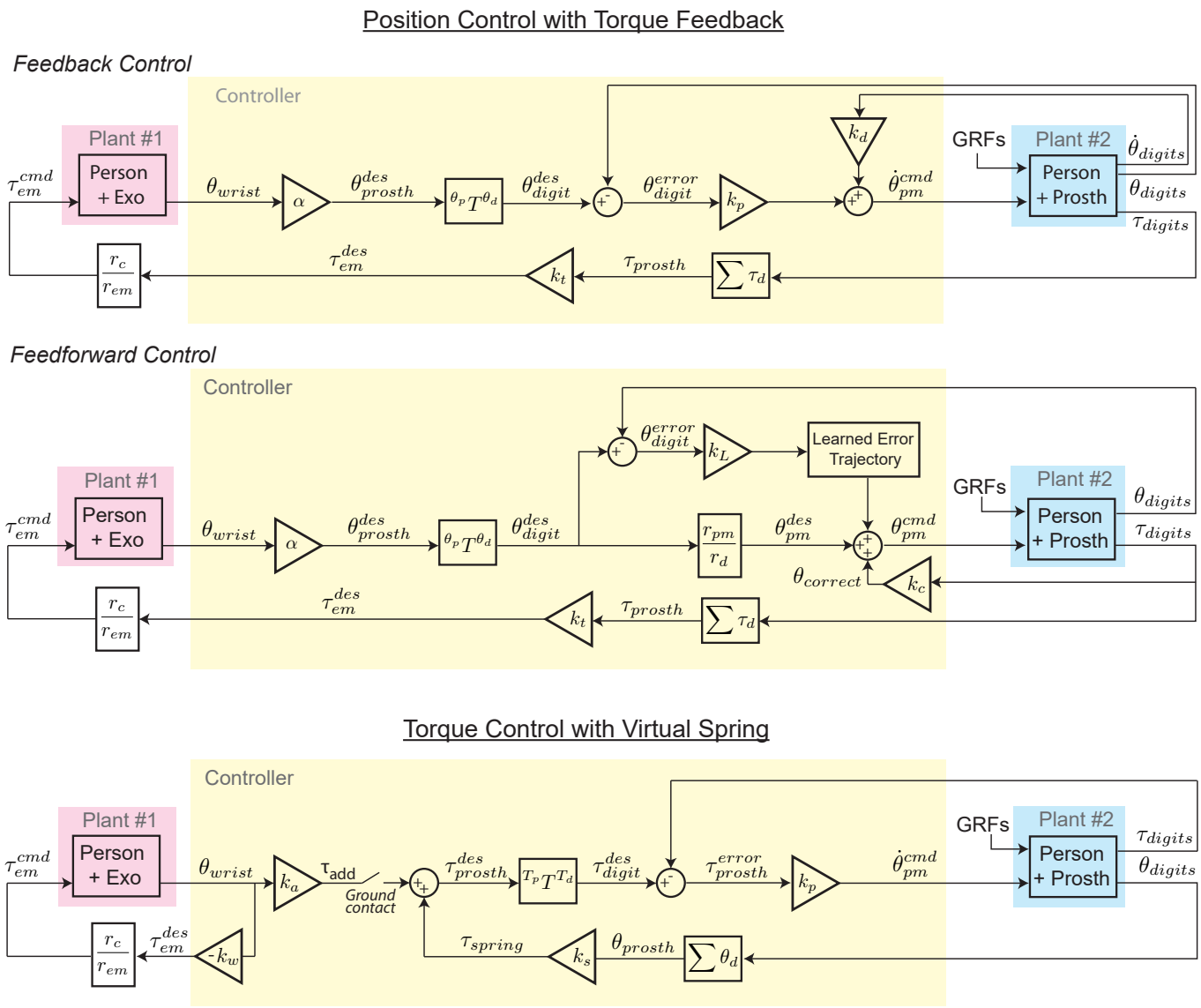

Fig. 3. Control block diagrams of both high-level control schemes, including both low-level controllers for the position control mode. The diagrams are simplified to only show the control of one of the three ankle prosthesis digits. In position control, the user directly controls the position of the prosthesis (Prosth) with the wrist exoskeleton (Exo). In feedback control, this is accomplished by using velocity control of the motor to minimize the errors in the desired angles. In feedforward control, this is accomplished by transforming a desired prosthesis angle to desired position of the motor drum that controls the Bowden cables, using model-based and model-free corrections. When haptic feedback is provided, a scaled version of the ankle prosthesis torque is fed back to the wrist exoskeleton for both controller types. In torque control, the user exerts force against a virtual spring in the wrist exoskeleton, which is transformed to an ankle torque added to a basic spring controller.

simultaneously receiving torque feedback from the ankle. Therefore, the user receives proprioceptive feedback about the angular position of the ankle via their wrist proprioception, efference copy (providing predicted sensation based on the motor command), and feedback at the wrist regarding the ankle torque. We compared the performance of two low-level controllers used to implement this scheme: (1) a feedback controller, and (2) a feedforward controller with torque compensation and iterative learning.

The ankle prosthesis has three degrees of freedom (the heel and two toes), while the user only commands one degree of freedom, so the user's wrist angle is mapped to a single commanded ankle angle. The wrist position command is first converted to a commanded ankle angle by multiplying by a scaling factor, α, because the typical range of motion of the wrist is much larger than the range of motion of the ankle. This commanded ankle angle is then translated to angular positions for each of the digits, using two additional constraints on the position: (1) a set offset between the two toe digits, and (2) a set overall height for the prosthesis, approximately equal to the height of the intact ankle joint of the user with amputation. Both the toe offset and the fixed height are determined with the help of a prosthetist during an initial evaluation session.

1) Feedback Position Control: In this low-level controller, the velocity commands sent to the motors controlling the ankle prosthesis digits ($\dot{\theta}_{pm}^{cmd}$) result from a modified proportional derivative (PD) controller with the wrist angle as input. Although the implemented control is complicated by the fact that each digit of the prosthesis is controlled separately to obtain the final ankle angle with the constraints listed above, the basic behavior can be described as follows:

$$\dot{\theta}_{pm}^{cmd} = k_p(\alpha\theta_{wrist} - \theta_{ankle}) + k_d(\dot{\theta}_{ankle}) \quad (1)$$

The proportional term k_p tracks the wrist angle at the ankle. The derivative term k_d is used to reduce overshoot and increase stability of the system. These gains were hand-tuned in order to achieve accuracy and stability. During the walking trial, the gains were set to a proportional k_p term of 20 and a derivative k_d term of 0.2.

2) Feedforward Position Control: In this low-level controller, the desired angle for each digit of the prosthesis is computed and translated into a desired position of the motor drum, θ_{pm}^{cmd}, which dictates the length of the Bowden cable controlling the prosthesis digit. Using the relationship between the radius of the prosthesis digit and the radius of the motor drum, along with the initial voltage commanded at a starting position, we determine the input voltage required to reach a desired position. The effect of elasticity of the Bowden cables and forces applied at the digits as the user walks on the prosthesis is compensated for using two correction terms: a model-based correction term and a model-free correction. The first term models each Bowden cable as a simple spring, resulting in a linear relationship between forces applied at the digits and resulting position errors. Therefore, this correction term of $k_c\tau_{digit}$ is added to the desired motor position. Because the simple linear model does not capture all errors, a second term provides model-free correction based on iterative learning. This additional learning term keeps a running average of the errors (e) accumulated at each timepoint in the gait cycle, which are used to apply a correction at each of those timepoints plus a pre-determined time delay throughout the gait cycle, multiplied by a learning gain, k_L. This iterative learning approach has been previously described and implemented in cyclic walking tasks [23], [38]. The following control equation is used for the position control of the ankle prosthesis at each digit:

$$\theta_{pm}^{cmd} = \theta_{pm}^{des} + k_c\tau_{digit} + k_L e(t + t_{delay})\theta_{digit}^{error} \quad (2)$$

3) Torque Feedback: For both low level position controllers, the wrist exoskeleton motor (em) can also receive scaled torque feedback from the ankle. To transmit this torque, we use a simple proportional gain with a scaling factor of k_t, to account for large torques at the ankle that would be unsafe and uncomfortable to transmit to the wrist:

$$\tau_{em}^{cmd} = k_t\tau_{prosth} \quad (3)$$

Because similar high-quality haptic devices have been shown to be effective in open-loop control [45], we use open-loop control for this feedback system following benchtop testing to ensure torque display accuracy similar to human torque perception accuracy.

B. Torque Control with Virtual Spring

In this control scheme, the ankle prosthesis tracks a simple spring controller, while the user has the ability to modulate ankle prosthesis torque using the wrist. The following control law dictates the behavior of the ankle prosthesis:

$$\tau_{prosth}^{des} = k_s\theta_{prosth} + k_a\theta_{wrist} \quad (4)$$

The k_s gain determines the stiffness of the spring that governs the baseline motion of the ankle prosthesis, while the k_a gain determines the magnitude of the additional torque added or subtracted by the motion of the user.

The low-level control of each digit of the prosthesis consists of a proportional feedback term in velocity control. This is governed by the following equation:

$$\dot{\theta}_{pm}^{cmd} = k_p\tau_{digit}^{error} \quad (5)$$

The haptic feedback provided in this control mode is a virtual spring implemented at the wrist, which provides increasing torque to the wrist the further the wrist is driven away from the zero position. This allows the user to feel a scaled version of the torque that they are adding or subtracting from the device, and demonstrates where the neutral (zero) position of the wrist exoskeleton lies. This virtual spring is governed by the following equation:

$$\tau_{em}^{cmd} = -k_w\theta_{wrist} \quad (6)$$

IV. Benchtop Testing

We performed benchtop testing of the behavior of both the wrist exoskeleton and ankle prosthesis when controlled as described in Section III. For each device and control mode, two benchtop tests were performed: (1) an accuracy test comparing commanded signals to output signals, and (2) a frequency response test to determine how the system behaves across various input frequencies. Novel characterization tests were performed for the position response of the ankle prosthesis emulator and the torque response of the wrist exoskeleton. The torque response of the ankle prosthesis emulator has been previously characterized [38], but we present it here as well for comparison.

Our target goals for control accuracy were as follows: (1) static accuracy within the threshold for human perception, and (2) dynamic accuracy within the threshold of human perception for input frequencies under 6 Hz. We chose 6 Hz because the majority of the frequency content is below this value during walking [46]. Because of this design goal, we present a sample trace of the input and output values at this frequency, in addition to static accuracy data and dynamic accuracy plots across all tested frequencies. In order to provide the most conservative estimate of performance, iterative learning was not used during benchtop testing for the feedforward condition.

A. Torque response of ankle prosthesis emulator

For torque response testing of the ankle prosthesis emulator, the end-effector was fixed in a rigid frame to prevent movement, as described in [38]. Although the testing for each digit was performed separately, the responses of all digits were identical, and therefore only one result is shown for each

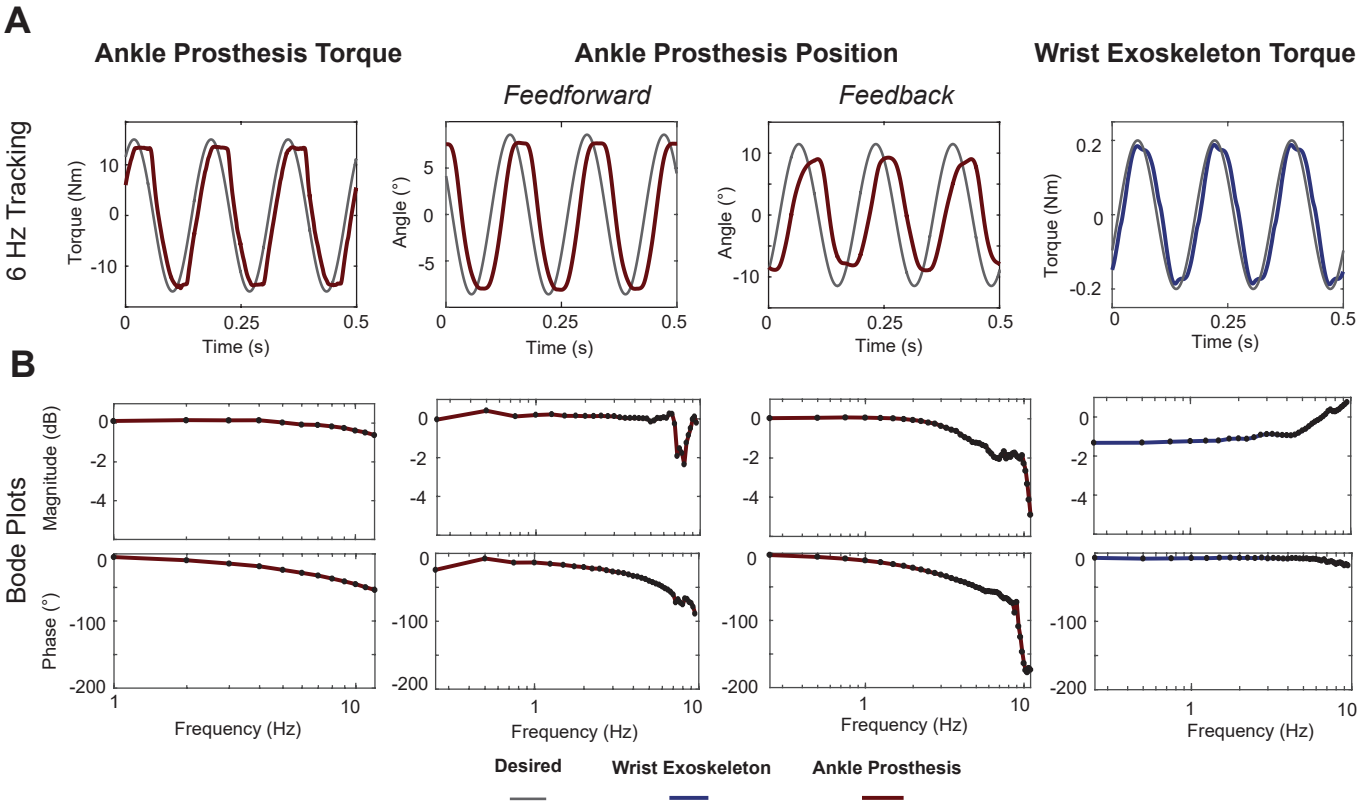

Fig. 4. Results from benchtop testing of both the ankle prosthesis and the wrist exoskeleton in each control mode: ankle prosthesis torque, ankle prosthesis position for both low-level controllers, and wrist exoskeleton torque. A. The majority of the frequency content in walking is below 6 Hz, and a sample trace at this frequency shows that the output signals track the desired curve with reasonable accuracy. B. Bode plots demonstrate that the bandwidth of each system that is greater than 6 Hz.

test. Measurement error was evaluated by comparing known applied torque to torque measured by the prosthesis emulator using strain gages. Root-mean-square (RMS) measurement error was 1.7 N·m. Up to 10 Hz, the magnitude and frequency response of the system had high fidelity, with the magnitude response degrading by less than 1 decibel and the phase lagging by less then $50°$ (Figure 4A). The response to a 6 Hz input is shown in Figure 4B.

B. Position response of ankle prosthesis emulator

For all position response characterization tests, the prosthesis was fixed in midair so that all digits could move freely. A position input combined with a set height was used to command all three digits simultaneously to result in an overall ankle angle proportional to the input. The proportional and derivative gains were held constant during all tests.

Within the position control scheme, encoders in each digit of the ankle prosthesis were used to determine the ankle angle. In order to validate the accuracy of the measured ankle angle, seven different angles were commanded to the prosthesis in a range of $-15°$ to $15°$, and the resulting encoder angle was compared to the angle determined by motion capture at 100 Hz (Vicon, United Kingdom). We repeated this sweep three times, and averaged to determine the final RMS error. In order to determine ankle angle using motion capture, we placed markers centered on the end of each digit, in addition to the testing rig base to determine the neutral zero angle. Ankle angle was calculated by finding the angle from the neutral angle to the plane consisting of the three end-effector markers. We also applied a uniform correction term so that the motion capture zero position matched the neutral ankle angle. The RMS error between the angle calculated by motion capture and the angle given by the encoders was found to be $0.0045°$, significantly less than human proprioceptive error for the ankle [47]. The same prosthesis encoders were used for both feedforward and feedback control.

To measure bandwidth, input frequencies up to 10 Hz were tested in increments of 0.25 Hz. Each frequency was commanded for 3 seconds, and the output was fit to a sine wave. The resulting amplitude and phase shift were used to generate a Bode plot. We define bandwidth as the lowest frequency during which the amplitude ratio drops below -3 dB or the phase margin exceeds $150°$. Based on these calculations, we determined the bandwidth to be 10 Hz for feedback control and greater than 10 Hz for feedforward control, both of which are greater than our target of 6 Hz (Figure 4B). The response to a 6 Hz input is shown in Figure 4A.

C. Torque response of wrist exoskeleton

To measure the accuracy and linearity of the motor torque applied to the wrist exoskeleton, we commanded a virtual spring centered around a neutral angle and hung masses of

known values from the wrist base, such that the further the motor traveled from the neutral position, the more resistance torque was applied. Each mass was allowed to reach steady state, and the motor torque commanded averaged. This averaged torque was compared to the known torque resulting from the mass hanging on the motor shaft with a known radius, compensating for the change in angle as a result of the displacement of the wrist base. This test was repeated in triplicate with 5 known masses. Both the wrist flexion and extension torque were tested by fixing the wrist exoskeleton upside-down in order to test the opposing direction. The resulting fit for the torque values was very linear, with an R^2 value of 0.996. In addition, the RMS error between commanded and actual torque was 0.0249 N·m (Figure 4A), a value similar to human torque discrimination in wrist flexion and extension [40].

An open-loop torque frequency response test was conducted using an external 6-axis Nano17 force/torque sensor (ATI Industrial Automation, North Carolina, USA). To conduct this test, a separate wrist exoskeleton was built identical to the original wrist exoskeleton, but which housed a force/torque sensor instead of the encoder in the opposite joint to the capstan drive. In addition, the main frame of the wrist exoskeleton was grounded in order to minimize movement during testing. This bandwidth test was also performed in triplicate with frequency increments of 0.25 Hz from 0.25 Hz to 10 Hz, and the resulting torque in the relevant direction was measured from the force/torque sensor. In the range of our testing frequencies, we did not reach the bandwidth of the system (Figure 4B). The response to a 6 Hz input is shown in Figure 4A.

V. Walking Trial

To test the system behavior during walking, we recruited one participant with a left-foot transtibial amputation (male, 44 years old, 2 years post-amputation) to walk with the devices. Prior to testing, the ankle-foot prosthesis was fit to the participant by a licensed prosthetist. All tests were done following a protocol approved by the Internal Review Board at Stanford University, and the participant gave written informed consent.

A. Experimental Protocol

The participant underwent a series of trials during which he used the wrist exoskeleton on his right wrist to control the ankle prosthesis on his left leg. Both high-level control schemes were tested: (1) position control and (2) torque control with a virtual wrist spring. We tested the high-level position control in separate trials both with and without haptic feedback. We also tested both low-level position controllers (feedback and feedforward), in addition to comparing the performance of the feedforward control with and without iterative learning. Testing was done over the course of two days. On the first day, we tested feedback position control with and without haptics, followed by torque control. On the second day, we tested feedforward position control, with and without iterative learning. All trials were five minutes long, except for one trial with feedforward position control and iterative learning and no haptic feedback. This trial produced spikes in the torque profile and was ended 30 seconds early to due to subject discomfort.

To acclimate to the system, the participant first practiced teleoperating the ankle prosthesis in position control without feedback while seated, then while standing, and finally while walking on a treadmill (Bertec, Ohio, USA). Next, torque feedback was turned on and the participant first acclimated to feedback at the wrist while standing and then while walking. This same training protocol was followed for both types of low-level position control. During feedforward position control, iterative learning was turned on only in the last 90 seconds of walking. We allowed the participant to first walk without iterative learning in order to establish consistent cyclic errors, and found that 3.5 minutes allowed the participant to achieve a consistent desired wrist, and thus ankle, trajectory. This allowed for effective error compensation using iterative learning. Finally, because the force feedback at the wrist was different in torque control compared to position control, the participant acclimated to the virtual spring at the wrist while seated before walking. We allowed the participant to self-select walking speed, which was between 0.8 m/s and 1.0 m/s across all trials.

B. Real-Time Feedback

In order to demonstrate that a person is able to voluntarily modulate the behavior of the ankle prosthesis using teleoperation control via the wrist exoskeleton, we provided two different trajectories for the user to follow in each training and testing condition. It has been previously demonstrated that humans can use real-time visual feedback to modulate their gait patterns [48], [49] and upper extremity movement [50]. However, studies instructing subjects to modulate their gait typically provide cues in the form of binary feedback, and studies in the upper extremity typically occur while participants are seated. Therefore, it was unclear whether a person could follow a specific continuous wrist trajectory in real-time while walking. In order to verify this, we measured the root mean square error between the desired and measured wrist trajectory for each trial. We chose to display the desired wrist trajectory instead of the desired prosthesis trajectory in order to separate the human error between desired and realized wrist motion from the error in the mechanical system (between desired ankle prosthesis angle or torque and realized angle or torque). In all conditions, the user was able to see a graphical display of the desired wrist trajectory and the real-time wrist angle. This real-time feedback was displayed on a 40-inch screen placed in front of the user while seated, standing, or walking on the treadmill.

The desired wrist trajectories given for the training conditions were different from the test conditions, both in pattern and mechanics of how they were displayed. In all training trials where the subject was seated or standing, the desired trajectories were sine waves of various amplitudes and frequencies. The horizontal axis of the displayed graph was based on time, and so the real-time feedback to the subject about the current state of the wrist was reset after a set time period.

The desired trajectories for the walking trials were based on previously published kinematic data from people without amputation [51]. For position control conditions, a simplified and scaled version of a typical ankle trajectory over a gait cycle was used, with various amounts of toe push-off for the different trials. Because of this, the horizontal axis used for the real-time feedback during this trial was percent gait cycle, and the graph reset once a new heel strike was detected. For the torque control condition, the user only had control of the ankle during the stance phase. Therefore, percent stance was used as the horizontal axis in the real-time feedback plot, and the graph was once again reset when a new heel strike was detected.

C. Analysis

We were interested in how well the participant was able to track desired wrist trajectories, in addition to how well the ankle-foot prosthesis tracked the desired output (angular position or torque). For each of these metrics, RMS error was first calculated for each gait cycle in the last 30 seconds of each trial. Then, in order to perform a balanced ANOVA with repeated measures from individual gait cycles, the trial that contained the fewest number of gait cycles was identified, and the amount of gait cycles used for all other conditions was shortened to this number as well. A two-way ANOVA was performed using one trial of each position control condition for the desired trajectory that was closest to a typical biological ankle trajectory. In this ANOVA, both the low-level position control and the haptic feedback conditions were used as independent variables. To test system performance, each gait cycle was treated as one independent trial. No statistical testing was performed for the human wrist tracking error because we only tested one participant; the errors were dependent on the order of conditions tested because the participant improved wrist position tracking over time.

D. Results

1) Human Wrist Control: The two desired wrist trajectories that we asked the participant to follow for each position control and torque control condition were very different, yet he was able to follow desired trajectories with an average RMS error of $1.55°$ on the second day. Figure 5 shows four example trajectories of desired and measured wrist angles from each gait cycle during both position control (Day 2) and torque control (Day 1). For the trajectory most similar to the biological ankle, averages of the RMS error in each gait cycle for the last 30 seconds of each condition are shown in Figure 6. Figure 7 shows the corresponding traces for each gait cycle and group averages. The participant improved their wrist position tracking between Day 1 and Day 2, but no statistical testing was performed to examine the signfiicance of this learning because only one participant was tested.

2) Prosthesis Position Control: For the trajectory most similar to the biological ankle, Figure 6 shows the RMS error for each control method in the haptic feedback and no haptic feedback condition. The individual traces for each gait cycle in the last 30 seconds of that condition, in addition to the resulting torque, are shown in Figure 7. The two-way ANOVA rejected the null hypothesis that the control conditions were the same ($F(1) = 454.5, p = 2.42 \times 10^{-58}$), in addition to rejecting the null hypothesis that the haptics conditions were the same ($F(2) = 60.8, p = 2.05 \times 10^{-12}$). There was also a significant interaction effect between the control conditions and haptic feedback conditions ($p = 9.47 \times 10^{-10}$), so we ran separate paired t-tests for each condition, using a Bonferroni correction to account for six multiple comparisons (α = 0.0083).

Paired t-tests comparing the haptic effect in each control

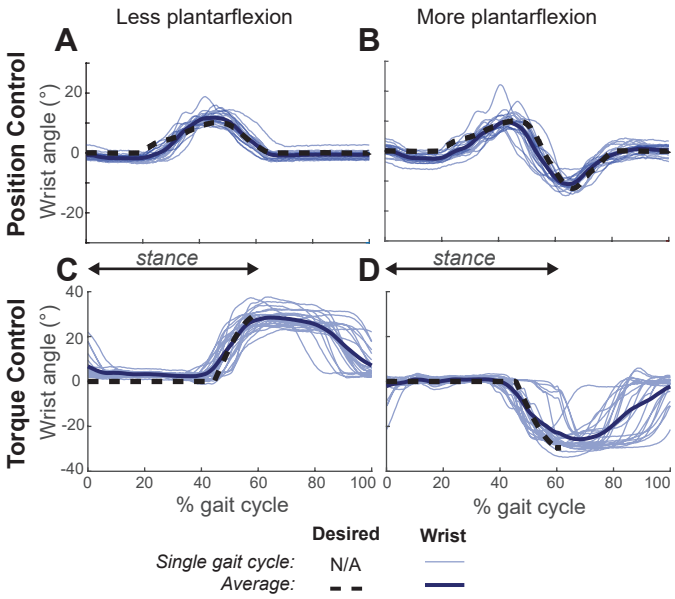

Fig. 5. Examples of the variety of desired and realized wrist angles for different trials. The top row shows examples of position control with the feedforward low-level controller with haptic feedback for the trajectory with less plantarflexion (A) and more plantarflexion (B). The bottom row shows examples of torque control with less plantarflexion torque (C) and more plantarflexion torque (D). The dashed line indicating the desired wrist trajectory ends in mid-stride for the bottom row because torque control was only active during the stance phase.

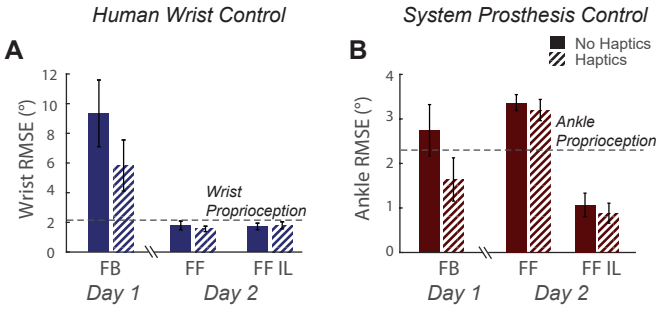

Fig. 6. Average and standard deviation of RMS error for wrist position and ankle position for the trajectory most similar to the biological ankle are shown for the three types of low-level position control, both with and without haptic feedback. A) Although the subject initially was not able to track the desired position very well, by Day 2 they consistently had low errors. B) The feedforward control with iterative learning (FF IL) performed best, followed by the feedback control (FB), and then the feedforward control without iterative learning (FF). There was also a significant difference between the haptics and no haptics conditions in the feedback controller.

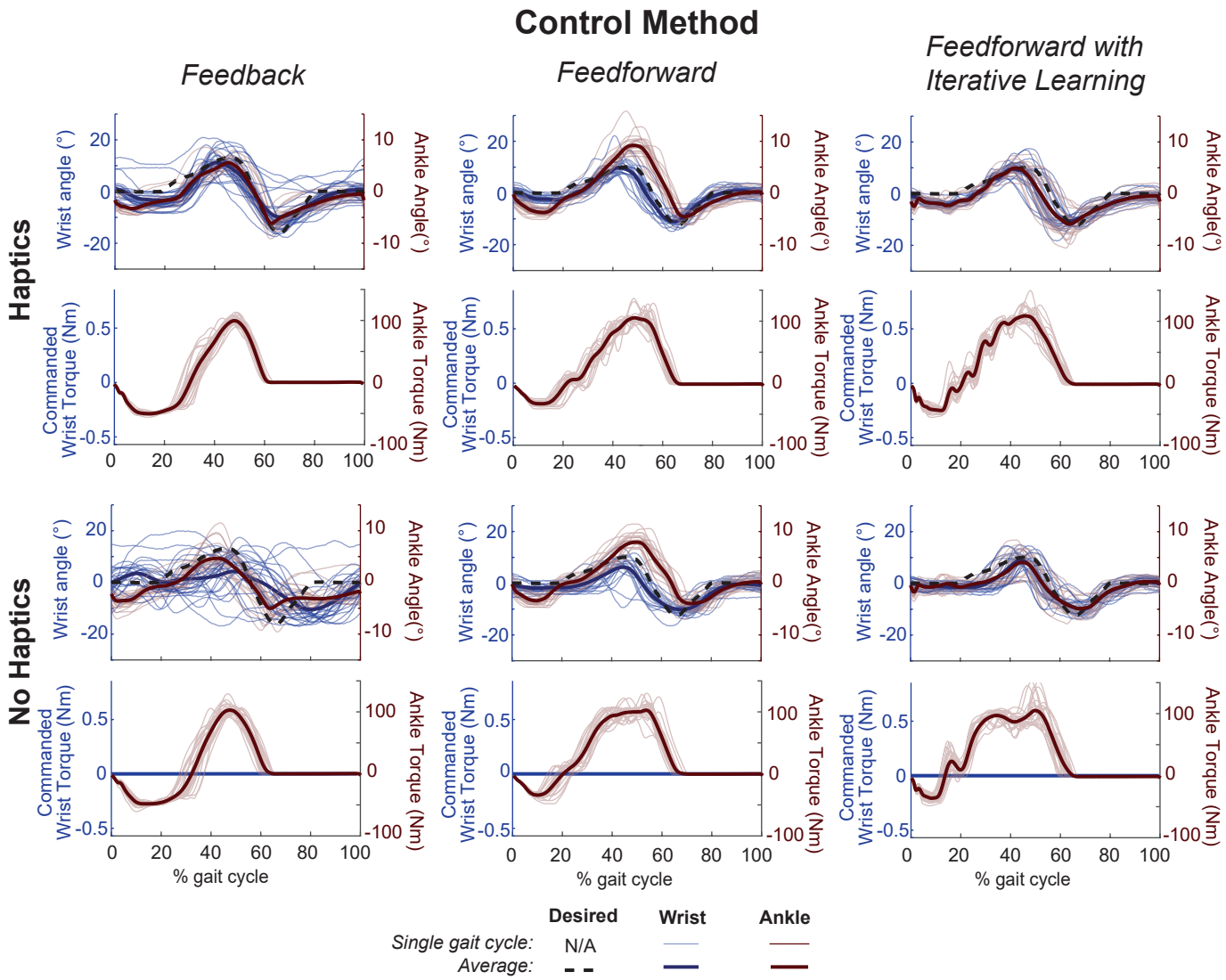

Fig. 7. Angle and torque of the wrist exoskeleton and ankle prosthesis for each position control condition. These representative data are from the final 30 seconds of trials in which the target trajectory was most similar to biological gait (the same trials as presented in Figure 6). For each condition, desired wrist trajectory, wrist position, and ankle position are shown in the top plot, and ankle torque and commanded wrist torque for the feedforward torque control are shown in the bottom plot. Because we used the previously characterized wrist exoskeleton properties to estimate wrist torque, the commanded wrist torque in the haptic feedback conditions exactly matches the scaled version of the ankle torque, and for this reason the traces of the wrist torque are not visible.

condition showed that the haptic feedback improved the feedback control ($p = 2.60 \times 10^{-6}$), but did not significantly improve the other two control conditions when the Bonferroni correction was taken into account (FF: $p = 0.0285$, FF IL: $p = 0.0251$, α = 0.0083). This explains the interaction effect.

Paired t-tests between each control condition, grouping the haptics and no haptics conditions together, confirmed that they were all significantly different from each other. The feedforward controller with iterative learning resulted in significantly lower error than the feedforward controller alone ($p = 1.36 \times 10^{-38}$) and the feedback controller ($p = 2.40 \times 10^{-13}$). The feedback controller also performed better than the feedforward controller alone ($p = 3.29 \times 10^{-12}$). Although the feedforward control condition with iterative learning performed the best, it also resulted in small oscillations in the resulting torque; these oscillations are not seen in the feedback controller (Figure 7).

3) Prosthesis Torque Control: Torque control fundamentally differs from position control in multiple ways. First, the prosthesis follows a baseline torque based on a virtual ankle spring. Therefore, the wrist exoskeleton only serves to modify this baseline trajectory, instead of having complete control of the trajectory as in the position control condition. Therefore, the desired wrist movement during torque control can be much simpler than the desired wrist movement during position control to acheive trajectories similar to the biological ankle. Another difference is that torque control was only active during stance, so desired trajectories were only provided during this time. Figure 8 shows the desired and measured wrist trajectories, in addition to the resulting ankle torque and position. As expected, the ankle plantarflexion torque increased when additional plantarflexion torque was commanded from the wrist exoskeleton. There is some error between the desired and measured torque (RMSE = 8.27 ± 1.46

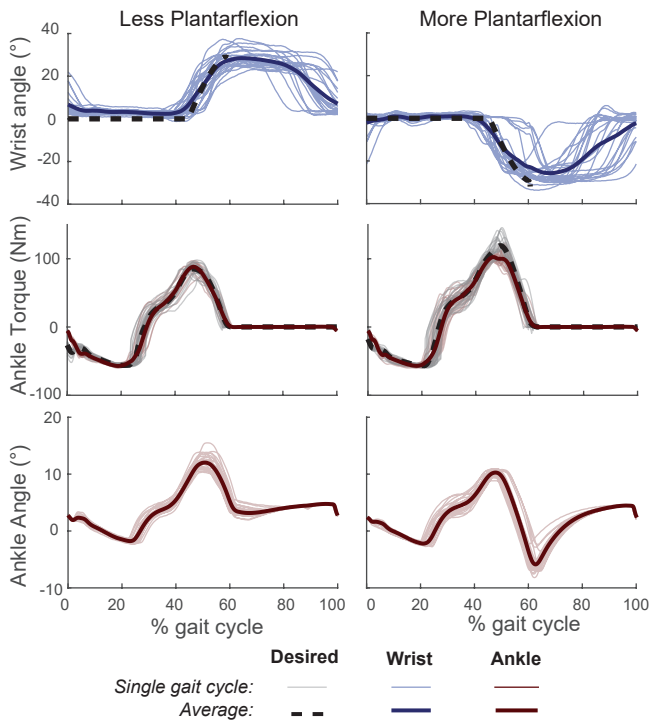

Fig. 8. Data from the torque control condition is shown, with the trial corresponding to less plantarflexion on the left and the trial corresponding to more plantarflexion on the right. The top row shows the desired and realized wrist trajectories, the middle row shows the commanded and measured torque from the prosthesis, and the bottom row shows the ankle position. The two trajectories produced different torque trajectories, although there was some error between desired and measured torque.

N·m), which could be corrected in the future with iterative learning, as in prior studies with this device [38].

VI. Discussion and Future Work

We developed a system that allows a user with a transtibial amputation to teleoperate their ankle-foot prosthesis and receive haptic feedback about the state of the prosthesis. A wrist exoskeleton senses wrist angle and implements wrist torque up to 1 Nm. Two different high-level teleoperation schemes allow the wrist exoskeleton to interface with the ankle prosthesis. The first directly controls the ankle prosthesis and receives wrist torques scaled to the prosthesis torques. The second modifies a spring-like torque trajectory with the wrist and receives haptic feedback proportional to the torque that the user inputs or removes from the system. Two different low-level controllers can be used for position control of the ankle prosthesis: feedback control and feedforward control with error corrections. A person with a transtibial amputation was able to effectively use the wrist exoskeleton to teleoperate the ankle prosthesis in real time using these control schemes.

Of the two control schemes tested, the position control provides the user with more information because they are able to feel a scaled version of the ankle torque at their wrist, in addition to using their intact wrist proprioception to estimate ankle angle. However, because the ankle prosthesis follows a scaled version of the wrist angle, the wrist movement needed to generate an ankle trajectory similar to the biological ankle is complex and therefore may result in greater cognitive load for the user. In contrast, the torque control scheme does not provide the user with as much information. The ankle prosthesis has a baseline behavior of a passive spring, and the user can inject or remove torque from this behavior via wrist movement. Because of the virtual spring at the wrist, the user can feel a scaled version of the torque that they are injecting or removing, but does not have a concrete representation of the overall torque or ankle position at any instant in time. While the user does not have as much information, the wrist trajectories required to generate a natural ankle trajectory can be much simpler. Additional control schemes could also be used for this system. For example, it would be possible for the ankle-foot prosthesis to behave autonomously while the user receives feedback at the wrist. In future work, functional gait metrics should be measured with the control approaches we have developed, as well as haptic feedback alone, to examine their individual effects. In addition, the differences between cognitive load or comfort of different control schemes could be tested.

In our teleoperation control schemes, we control the behavior of two separate devices: the wrist exoskeleton and the ankle prosthesis. Yet because both devices are attached to the human user, the system actually has two plants that are each a combination of the device and the limb to which they are attached: (1) the wrist exoskeleton and the wrist, including all of the musculature, proprioceptive organs, and neural commands to and from the wrist, and (2) the ankle-foot prosthesis and the musculature, priopriocepive organs, and neural commands from the residual limb and rest of the body that affect gait and therefore ground reaction forces. Accurate control of the prosthesis depends not only on the mechatronic system capabilities, but also on the capability of the user to accurately control their wrist in real time while they are walking. We found that, by the second day of training, our participant was able to match multiple desired trajectories with an error similar to that of proprioceptive acuity at the wrist. Because this was a proof-of-concept study with one participant, further work is required to generalize these results and characterize human adaptation to the system.

We were able to achieve sufficient control accuracy with this system, with ankle position RMS errors of less than 1° with the feedforward control with iterative learning. However, with this control strategy we noticed small oscillations in ankle torque not present with the feedback control, especially with haptic feedback present. It is unclear whether this is due to higher position tracking accuracy of the system or a by-product of this controller with torque compensation. Other teleoperation systems have noted a trade-off between higher tracking accuracy and this type of oscillatory behavior [33]. Future work will examine this possible trade-off between position control accuracy and torque oscillations, specifically whether these oscillations still exist if iterative learning is applied to feedback control instead of feedforward control. Additionally, it is unclear if perfect position tracking should be the desired goal of the system. If the ankle tracks position perfectly, it loses spring-like behavior, which could be uncomfortable for the user, especially if they are still learning how to accurately

control the wrist exoskeleton. We avoid this challenge with the torque control we implemented.

In the long term, we aim to use this system to test what users want from their prosthesis. Parameters for active prosthesis control have typically been hand-tuned to a generic control mode intended to work for an average user. However, customization using methods such as human-in-the-loop optimization (HILO) can substantially improve the efficacy of assistive devices [23]. We expect the same to be true for prostheses, but have not yet been successful, perhaps because the user has little sensory feedback to inform how they should best take advantage of each control law presented by the optimization system. We plan to test this system with HILO to determine whether the outcomes for functional gait metrics such as metabolic cost can be improved. In addition, because humans have been shown to continuously optimize metabolic cost [52], it is possible that the user could generate beneficial ankle trajectories with their wrist that are vastly different than those applied here, which were based on movements of the biological ankle.

There are many other scientific questions this novel teleoperation system could be used to address. For example, are people best able to operate the wrist exoskeleton with their dominant or non-dominant hand? Or, is it easier to learn using the wrist ipsilateral or contralateral to the amputation? Future work will address these questions. Systems like this could also be expanded in the future to incorporate an additional degree of freedom for medio-lateral stability, or untethered versions built to test for potential benefits during overground walking.

TABLE I
VARIABLES AND PARAMETERS

α	Scaling factor from wrist to ankle prosthesis angle
r_c	Wrist exoskeleton capstan radius
r_d	Ankle prosthesis digit radius
r_{em}	Wrist exoskeleton motor radius
r_{pm}	Ankle prosthesis motor radius
k_a	Added torque from user gain
k_c	Torque-based position compensation gain
k_L	Iterative learning gain
k_p	Proportional gain
k_d	Derivative gain
k_t	Torque feedback scaling gain
k_w	Wrist virtual spring gain
${}^{\theta_p}T^{\theta_d}$	Transformation from ankle prosthesis to digit angle
${}^{\tau_p}T^{\tau_d}$	Transformation from ankle prosthesis to digit torque
θ^{des}_{prosth}	Desired prosthesis angle
θ^{des}_{digit}	Desired prosthesis digit angle
θ^{des}_{pm}	Desired prosthesis motor angle
θ^{cmd}_{pm}	Commanded prosthesis motor angle
θ^{error}_{digit}	Error between desired and measured prosthesis digit angle
$\dot{\theta}^{des}_{pm}$	Desired prosthesis motor velocity
$\dot{\theta}^{cmd}_{pm}$	Commanded prosthesis motor velocity
τ_{add}	Torque added to prosthesis by user input
τ_{spring}	Spring torque command of prosthesis
τ^{des}_{prosth}	Desired prosthesis torque
τ^{des}_{digit}	Desired prosthesis digit torque
τ^{error}_{digit}	Error between desired and measured prosthesis digit torque

VII. CONCLUSION

Our system closes the loop on both the control and sensory feedback from a robotic ankle-foot prosthesis via a novel wrist exoskeleton and teleoperation scheme. Benchtop tests of all system components confirm sufficient accuracy and responsiveness. We also demonstrate the feasibility of the system by confirming that a subject with a transtibial amputation can volitionally control the ankle prosthesis in different ways while walking, and that the system can control ankle prosthesis position accurately under these conditions. Future work will further examine this system with additional participants and examine its effects on functional gait metrics such as metabolic cost, phantom limb pain, and balance.

ACKNOWLEDGMENT

The authors would like to thank our participant for his time and Susan Stenman, CP, for assisting us in fitting the prosthesis to our participant. We also thank Scott Delp for helpful insights and high-level feedback, as well as Laura Blumenschein, Margaret Koehler, Cole Simpson, and other members of the Collaborative Haptics and Robotics in Medicine Lab and the Stanford Biomechatronics Lab for their help with debugging, statistics, and editing. This work was funded by an National Science Foundation Graduate Research Fellowship to CGW (DGE-1656518) and an National Science Foundation GARDE Grant (CBET-1511177).

REFERENCES

[1] K. Ziegler-Graham, E. J. MacKenzie, P. L. Ephraim, T. G. Travison, and R. Brookmeyer, "Estimating the Prevalence of Limb Loss in the United States: 2005 to 2050," *Archives of Physical Medicine and Rehabilitation*, vol. 89, no. 3, pp. 422–429, 2008.

[2] J. M. McGavock, N. D. Eves, S. Mandic, N. M. Glenn, H. A. Quinney, and M. J. Haykowsky, "The Role of Exercise in the Treatment of Cardiovascular Disease Associated with Type 2 Diabetes Mellitus," *Sports Medicine*, vol. 34, no. 1, pp. 27–48, 2004.

[3] C. T. Huang, J. R. Jackson, N. B. Moore, P. R. Fine, K. V. Kuhlemeier, G. H. Traugh, and P. T. Saunders, "Amputation: energy cost of ambulation." *Archives of Physical Medicine and Rehabilitation*, vol. 60, no. 1, pp. 18–24, 1979.

[4] N. H. Molen, "Energy/speed relation of below-knee amputees walking on a motor-driven treadmill," *Internationale Zeitschrift für Angewandte Physiologie Einschließlich Arbeitsphysiologie*, vol. 31, no. 3, pp. 173–85, 1973.

[5] K. Hagberg and R. Brånemark, "Consequences of non-vascular transfemoral amputation: A survey of quality of life, prosthetic use and problems," *Prosthetics and Orthotics International*, vol. 25, no. 3, pp. 186–194, 2001.

[6] R. Gailey, K. Allen, J. Castles, J. Kucharik, and M. Roeder, "Review of secondary physical conditions associated with lower-limb amputation and long-term prosthesis use," *The Journal of Rehabilitation Research and Development*, vol. 45, no. 1, pp. 15–29, 2007.

[7] P. Ephraim and L. Duncan, "People with Amputation Speak Out With the Amputee Coalition of America," Johns Hopkins Bloomberg School of Public Health, Baltimore, MD, Tech. Rep., 2014.

[8] W. C. Miller, M. Speechley, and B. Deathe, "The prevalence and risk factors of falling and fear of falling among lower extremity amputees," *Archives of Physical Medicine and Rehabilitation*, vol. 82, no. 8, pp. 1031–1037, 2001.

[9] G. Bergen, M. R. Stevens, and E. R. Burns, "Falls and Fall Injuries Among Adults Aged 65 Years — United States, 2014," *Morbidity and Mortality Weekly Report*, vol. 63, no. 17, pp. 379–83, 2016.

[10] P. A. Struyf, C. M. van Heugten, M. W. Hitters, and R. J. Smeets, "The Prevalence of Osteoarthritis of the Intact Hip and Knee Among Traumatic Leg Amputees," *Archives of Physical Medicine and Rehabilitation*, vol. 90, no. 3, pp. 440–6, 2009.

[11] D. C. Norvell, J. M. Czerniecki, G. E. Reiber, C. Maynard, J. A. Pecoraro, and N. S. Weiss, "The prevalence of knee pain and symptomatic knee osteoarthritis among veteran traumatic amputees and nonamputees," *Archives of Physical Medicine and Rehabilitation*, vol. 86, no. 3, pp. 487–93, 2005.

[12] C. T. Fuentes and A. J. Bastian, "Where Is Your Arm? Variations in Proprioception Across Space and Tasks," *Journal of Neurophysiology*, vol. 103, no. 1, pp. 164–171, 2010.

[13] C. Tong and J. R. Flanagan, "Task-Specific Internal Models for Kinematic Transformations," *Journal of Neurophysiology*, vol. 90, no. 2, pp. 578–85, 2003.

[14] M. D'Alonzo and C. Cipriani, "Vibrotactile Sensory Substitution Elicits Feeling of Ownership of an Alien Hand," *PLoS ONE*, vol. 7, no. 11, p. e50756, 2012.

[15] C. Dietrich, S. Nehrdich, S. Seifert, K. R. Blume, W. H. R. Miltner, G. O. Hofmann, and T. Weiss, "Leg Prosthesis With Somatosensory Feedback Reduces Phantom Limb Pain and Increases Functionality." *Frontiers in Neurology*, vol. 9, p. 270, 2018.

[16] F. M. Petrini, M. Bumbasirevic, G. Valle, V. Ilic, P. Mijović, P. Čvančara, F. Barberi, N. Katic, D. Bortolotti, D. Andreu, K. Lechler, A. Lesic, S. Mazic, B. Mijović, D. Guiraud, T. Stieglitz, A. Alexandersson, S. Micera, and S. Raspopovic, "Sensory feedback restoration in leg amputees improves walking speed, metabolic cost and phantom pain," *Nature Medicine*, vol. 25, no. 9, pp. 1356–1363, 2019.

[17] T. R. Clites, M. J. Carty, J. B. Ullauri, M. E. Carney, L. M. Mooney, J. F. Duval, S. S. Srinivasan, and H. M. Herr, "Proprioception from a neurally controlled lower-extremity prosthesis," *Science Translational Medicine*, vol. 10, no. 443, 2018.

[18] C. E. Stepp and Y. Matsuoka, "Relative to direct haptic feedback, remote vibrotactile feedback improves but slows object manipulation," in *International Conference of the IEEE Engineering in Medicine and Biology Society*, 2010, pp. 2089–92.

[19] B. Gillespie, J. Baker, M. O'Malley, P. Shewokis, and J. L. Contreras-Vidal, "Functionally biarticular control for smart prosthetics," in *World Haptics*, 2009, pp. 627–628.

[20] A. Panarese, B. Edin, F. Vecchi, M. Carrozza, and R. Johansson, "Humans Can Integrate Force Feedback to Toes in Their Sensorimotor Control of a Robotic Hand," *IEEE Transactions on Neural Systems and Rehabilitation Engineering*, vol. 17, no. 6, pp. 560–567, 2009.

[21] S. Au, J. Weber, and H. Herr, "Powered Ankle–Foot Prosthesis Improves Walking Metabolic Economy," *IEEE Transactions on Robotics*, vol. 25, no. 1, pp. 51–66, 2009.

[22] H. M. Herr and A. M. Grabowski, "Bionic ankle-foot prosthesis normalizes walking gait for persons with leg amputation." *Proceedings of Biological Sciences*, vol. 279, no. 1728, pp. 457–64, 2012.

[23] J. Zhang, C. Chern Cheah, and S. H. Collins, "Experimental comparison of torque control methods on an ankle exoskeleton during human walking," in *IEEE International Conference on Robotics and Automation*, 2015, pp. 5584–89.

[24] L. J. Hargrove, A. M. Simon, A. J. Young, R. D. Lipschutz, S. B. Finucane, D. G. Smith, and T. A. Kuiken, "Robotic leg control with EMG decoding in an amputee with nerve transfers," *New England Journal of Medicine*, vol. 369, pp. 1237–42, 2013.

[25] T. R. Clites, H. M. Herr, S. S. Srinivasan, A. N. Zorzos, and M. J. Carty, "The Ewing amputation: The first human implementation of the agonist-antagonist myoneural interface," *Plastic and Reconstructive Surgery – Global Open*, vol. 6, no. 11, p. e1997, 2018.

[26] S. K. Au, P. Bonato, and H. Herr, "An EMG-position controlled system for an active ankle-foot prosthesis: An initial experimental study," in *IEEE International Conference on Rehabilitation Robotics*, 2005, pp. 375–379.

[27] J. Wang, O. A. Kannape, and H. M. Herr, "Proportional EMG control of ankle plantar flexion in a powered transtibial prosthesis," in *IEEE International Conference on Rehabilitation Robotics*, 2013.

[28] S. Huang, J. P. Wensman, and D. P. Ferris, "Locomotor Adaptation by Transtibial Amputees Walking with an Experimental Powered Prosthesis under Continuous Myoelectric Control," *IEEE Transactions on Neural Systems and Rehabilitation Engineering*, vol. 24, no. 5, pp. 573–581, 2016.

[29] G. Niemeyer, C. Preusche, and G. Hirzinger, "Chapter 31: Telerobotics," in *Springer Handbook of Robotics*, B. Siciliano and O. Khatib, Eds. Springer, 2008, pp. 741–747.

[30] B. Hannaford, "Stability and performance tradeoffs in bi-lateral telemanipulation," in *IEEE International Conference on Robotics and Automation*, 1989, pp. 1764–1767.

[31] K. Hashtrudi-Zaad and S. E. Salcudean, "Analysis of Control Architectures for Teleoperation Systems with Impedance/Admittance Master and Slave Manipulators," *The International Journal of Robotics Research*, vol. 20, no. 6, pp. 419–445, 2001.

[32] A. Gijsberts, R. Bohra, D. Sierra González, A. Werner, M. Nowak, B. Caputo, M. A. Roa, and C. Castellini, "Stable myoelectric control of a hand prosthesis using non-linear incremental learning," *Frontiers in Neurorobotics*, vol. 8, p. 8, 2014.

[33] A. M. Okamura, "Haptic feedback in robot-assisted minimally invasive surgery," *Current Opinion in Urology*, vol. 19, no. 1, pp. 102–107, 2009.

[34] O. Mohareri, S. E. Salcudean, and C. Nguan, "Asymmetric force feedback control framework for teleoperated robot-assisted surgery," in *IEEE International Conference on Robotics and Automation*, 2013.

[35] P. S. Lum, C. G. Burgar, M. V. der Loos, P. C. Shor, M. Majmundar, and R. Yap, "MIME robotic device for upper-limb neurorehabilitation in subacute stroke subjects: A follow-up study," *The Journal of Rehabilitation Research and Development*, vol. 43, no. 5, pp. 631–42, 2006.

[36] K. Karunakaran, K. Abbruzzese, Hao Xu, N. Ehrenberg, and R. Foulds, "Haptic proprioception in a virtual locomotor task," in *International Conference of the IEEE Engineering in Medicine and Biology Society*, 2014, pp. 3594–3597.

[37] F. R. Willett, D. R. Deo, D. T. Avansino, P. Rezaii, L. Hochberg, J. Henderson, and K. Shenoy, "Hand Knob Area of Motor Cortex in People with Tetraplegia Represents the Whole Body in a Modular Way," *Cell*, vol. 181, no. 2, pp. 396–409, 2020.

[38] V. L. Chiu, A. Voloshina, and S. Collins, "An Ankle-Foot Prosthesis Emulator Capable of Modulating Center of Pressure." *IEEE Transactions on Biomedical Engineering*, vol. 67, no. 1, pp. 166–76, 2020.

[39] Y. Yoshii, H. Yuine, O. Kazuki, W. lin Tung, and T. Ishii, "Measurement of wrist flexion and extension torques in different forearm positions," *BioMedical Engineering OnLine*, vol. 14, no. 1, p. 115, 2015.

[40] M. Vicentini, S. Galvan, D. Botturi, and P. Fiorini, "Evaluation of Force and Torque Magnitude Discrimination Thresholds on the Human Hand-Arm System," *ACM Transactions on Applied Perception*, vol. 8, no. 1, 2010.

[41] D. C. Boone and S. P. Azen, "Normal range of motion of joints in male subjects," *Journal of Bone and Joint Surgery – Series A*, vol. 61, no. 5, pp. 756–9, 1979.

[42] L. Cappello, N. Elangovan, S. Contu, S. Khosravani, J. Konczak, and L. Masia, "Robot-Aided Assessment of Wrist Proprioception," *Frontiers in Human Neuroscience*, vol. 9, p. 198, 2015.

[43] S. Contu, L. Cappello, J. Konczak, and L. Masia, "Preliminary analysis of non-dominant proprioceptive acuity and interlimb asymmetry in the human wrist," in *International Conference of the IEEE Engineering in Medicine and Biology Society*, 2015, pp. 3598–3601.

[44] F. Marini, V. Squeri, P. Morasso, J. Konczak, and L. Masia, "Robot-Aided Mapping of Wrist Proprioceptive Acuity across a 3D Workspace," *PLOS ONE*, vol. 11, no. 8, p. e0161155, 2016.

[45] D. Feygin, "Kinematics and Dynamics of Phantom (TM) model 1.5 Haptic Interface," Tech. Rep., 2001. [Online]. Available: http://citeseerx.ist.psu.edu/viewdoc/summary?doi=10.1.1.19.7619

[46] D. A. Winter, H. G. Sidwall, and D. A. Hobson, "Measurement and reduction of noise in kinematics of locomotion," *Journal of Biomechanics*, vol. 7, no. 2, pp. 157–9, 1974.

[47] N. Deshpande, D. M. Connelly, E. G. Culham, and P. A. Costigan, "Reliability and validity of ankle proprioceptive measures," *Archives of Physical Medicine and Rehabilitation*, vol. 84, pp. 883–9, 2003.

[48] J. C. van den Noort, F. Steenbrink, S. Roeles, and J. Harlaar, "Real-time visual feedback for gait retraining: toward application in knee osteoarthritis," *Medical and Biological Engineering and Computing*, vol. 53, pp. 275–86, 2015.

[49] H. P. Crowell and I. S. Davis, "Gait retraining to reduce lower extremity loading in runners," *Clinical Biomechanics*, vol. 26, no. 1, pp. 78–83, 2011.

[50] J. A. Saunders and D. C. Knill, "Humans use continuous visual feedback from the hand to control fast reaching movements," *Experimental Brain Research*, vol. 152, no. 3, pp. 341–52, 2003.

[51] E. M. Arnold, S. R. Hamner, A. Seth, M. Millard, and S. L. Delp, "How muscle fiber lengths and velocities affect muscle force generation as humans walk and run at different speeds," *Journal of Experimental Biology*, vol. 216, no. 11, pp. 2150–60, 2013.

[52] J. C. Selinger, S. M. O'Connor, J. D. Wong, and J. M. Donelan, "Humans Can Continuously Optimize Energetic Cost during Walking," *Current Biology*, vol. 25, no. 18, pp. 2452–2456, 2015.